Low-frequency noise in junctionless multigate transistors

Doyoung Jang, Jae Woo Lee, Chi-Woo Lee, Jean-Pierre Colinge, Laurent Montès' , Jung Il Lee, Gyu Tae Kim' , and Gérard Ghibaudo

Citation: Appl. Phys. Lett. **98**, 133502 (2011); doi: 10.1063/1.3569724
View online: http://dx.doi.org/10.1063/1.3569724
View Table of Contents: http://aip.scitation.org/toc/apl/98/13
Published by the American Institute of Physics

Low-frequency noise in junctionless multigate transistors

Doyoung Jang,[1,2,3] Jae Woo Lee,[2,3] Chi-Woo Lee,[4] Jean-Pierre Colinge,[4] Laurent Montès,[2,a)] Jung Il Lee,[1] Gyu Tae Kim,[3,b)] and Gérard Ghibaudo[2]
[1]*Korea Institute of Science and Technology, Sungbuk-gu, Seoul 136-791, Republic of Korea*
[2]*IMEP-LAHC, Grenoble INP-MINATEC, 3 Parvis Louis Néel, 38016 Grenoble, France*
[3]*School of Electrical Engineering, Korea University, Seoul 136-701, Republic of Korea*
[4]*Tyndall National Institute, University College Cork, Lee Maltings, Cork, Ireland*

(Received 7 February 2011; accepted 3 March 2011; published online 28 March 2011)

Low-frequency noise in n-type junctionless multigate transistors was investigated. It can be well understood with the carrier number fluctuations whereas the conduction is mainly limited by the bulk expecting Hooge mobility fluctuations. The trapping/release of charge carriers is related not only to the oxide-semiconductor interface but also to the depleted channel. The volume trap density is in the range of $6-30\times10^{16}$ $cm^{-3}\,eV^{-1}$, which is similar to $Si-SiO_2$ bulk transistors and remarkably lower than in high-k transistors. These results show that the noise in nanowire devices might be affected by additional trapping centers. © *2011 American Institute of Physics*.
[doi:10.1063/1.3569724]

Measurement of low-frequency (LF) noise in electronic devices is a powerful technique for studying the electrical transport and evaluating the device interface quality. The LF noise is known to be attributed to either Hooge mobility fluctuations (HMFs) or to carrier number fluctuations (CNFs) depending on the prevalence of the bulk or the surface conduction, respectively.[1,2] In metal-oxide-semiconductor field effect transistors (MOSFETs), which are generally operated in inversion-mode (surface conduction), the CNFs stem from carrier trapping/release at oxide-semiconductor interface, whereas the HMFs could prevail for bulk operated devices.[3–5] Recently, a proposed device without any junctions between the channel and the source/drain, called the "junctionless transistor" (JLT) has been proposed to overcome some issues such as short-channel effects.[6] The JLT is fully depleted below threshold. Above threshold the current flows through the bulk of the silicon, and an accumulation channel can be formed if the gate voltage is increased to sufficiently large values.[7] It has some advantages over surface-channel devices; less degradation of the mobility and near-ideal subthreshold slope.[8,9] In this paper, we report the LF noise behavior in an n-type JLT in which the drain current mainly flows through a bulk channel. An additional conduction was considered in a lightly accumulated channel when the gate voltage is large enough.

A device schematic and a cross-sectional view of an n-type JLT are shown in Fig. 1(a) (insets). JLTs were fabricated on a standard Unibond® silicon-on-insulator substrate. The top silicon layer was thinned down to a thickness of 5–10 nm and multigate structured nanowires were patterned by electron-beam lithography. The fin widths (W_{fin}) of the nanowires were defined from 30, 40, and 50 nm. A 10-nm-thick SiO_2 gate oxide was then thermally grown, such that each W_{fin} was reduced by approximately 10 nm to values of 20, 30, and 40 nm. Owing to the etching and oxidation process, the devices have an omega-gate structure. The nanowires were uniformly n^+ doped ($1-2\times10^{19}$ cm^{-3}) by ion implantation (channel, source, and drain). To achieve the full depletion of the channel for the off-state, a p^+ polysilicon gate electrode was used (work function=5.25 eV). The channel length is 1 μm.

Static and noise measurement were simultaneously performed in a dark box at room temperature. The back gate (substrate) was grounded. Typical transfer characteristics (I_d-V_g curves) in the linear regime (V_d=50 mV) with different values of W_{fin} are shown in Fig. 1(a). When the device is turned off, the n^+ doped channel is fully depleted by the

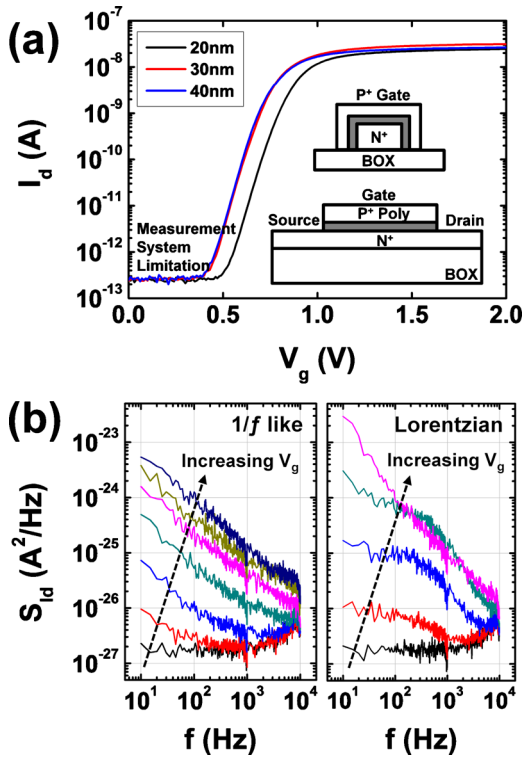

FIG. 1. (Color online) (a) I_d-V_g characteristics with different W_{fin} at V_d =50 mV. A device schematic and a cross-section view of a JLT (inset). (b) Drain current noise power spectrum (S_{Id}) as a function of the frequency for V_g varying from 0.2 to 2.0 V. They exhibit $1/f$-like (left) or Lorentzian (right) noise depending on the samples.

a)Electronic mail: laurent.montes@minatec.inpg.fr.
b)Electronic mail: gtkim@korea.ac.kr.

difference of the work function between the p^+ doped gate electrode and the channel. The estimated flat-band voltage $[V_{fb}=(E_{F\_channel}-E_{F\_gate})/q]$ is approximately 1–1.1 V. When V_g is increased, the depletion region in the channel is gradually removed and an un-depleted (neutral) n^+ channel is formed in the center of the device. Moreover, when $V_g > V_{fb}$, an accumulation channel is added to the total conduction. The largest part of the current in the JLTs is due to bulk conduction, but the formation of a surface accumulation channel is also observed at high V_g.

From the LF noise measurement, the drain current noise power spectrum (S_{Id}) was obtained as changing V_g between 10 Hz and 10 kHz as shown in Fig. 1(b). The noise exhibits, depending on the samples, a $1/f$ like (left) or Lorentzian (right) behavior in the subthreshold region, converging to essentially $1/f$ noise above the threshold region. For HMF, the LF noise can be described by the following empirical relationship:

$$\frac{S_{Id}}{I_d^{\beta}} = \frac{\alpha_H}{N_c}\frac{1}{f^{\gamma}} = \frac{q\alpha_H \mu_{bulk} V_d}{f^{\gamma} I_d L^2}, \tag{1}$$

where $I_d(=qN_c\mu_{bulk}V_d/L^2)$ is the drain current (A), α_H the Hooge constant, N_c the total number of charge carriers, f the frequency (Hz), μ_{bulk} the bulk mobility (cm^2/Vs), L the channel length, and β, γ the scaling exponents. The scaling exponents are estimated to be 2 and 1, respectively. There are two models to explain the origin of the LF noise; one is the HMF model defined by Eq. (1) and the other is based on the number fluctuation of charge carriers correlated with mobility fluctuations (CNF+CMF).[5,10] The mobility fluctuations are due to Coulombic scattering by trapped charges. Unlike the HMF model for bulk conduction, the CNF+CMF model is well defined for surface conduction, and the noise can be expressed by,

$$\frac{S_{Id}}{I_d^2} = S_{Vfb}\cdot\left(1+\alpha_C\mu_{eff}C_{ox}\frac{I_d}{g_m}\right)^2\cdot\left(\frac{g_m}{I_d}\right)^2, \tag{2}$$

where S_{Vfb} is the flat-band voltage power spectrum (V^2/Hz), α_C the Coulomb scattering parameter which is relevant to mobility fluctuations (Vs/C), μ_{eff} the effective mobility (cm^2/Vs), C_{ox} the oxide capacitance per unit area (F/cm^2), and g_m $(=\delta I_d/\delta V_g)$ the transconductance. The S_{Vfb} arises from tunneling process at the oxide interface:

$$S_{Vfb} = \frac{q^2 k_B T \lambda N_t}{fWLC_{ox}^2}, \tag{3}$$

where q is the electronic charge, k_B the Boltzmann constant, T the temperature (K), λ the oxide tunneling length (cm), N_t the volume oxide trap density ($cm^{-3}\,eV^{-1}$), and W the total channel width. These equations indicate that the normalized noise spectrum (S_{Id}/I_d^2) is proportional to $1/I_d$ in the HMF model whereas it varies as $(g_m/I_d)^2$ in the CNF+CMF model.

To identify the noise source, S_{Id}/I_d^2 is plotted in a log-log scale as a function of I_d in Fig. 2(a). The noise spectrum predicted by the CNF+CMF model is verified over a large current range, both below and above threshold. The noise predicted by the HMF model is also shown by the straight dashed line in Fig. 2(a). It is clearly not able to explain the LF noise dependence on drain current from below to above threshold region. Figure 2(a) clearly indicates that the noise

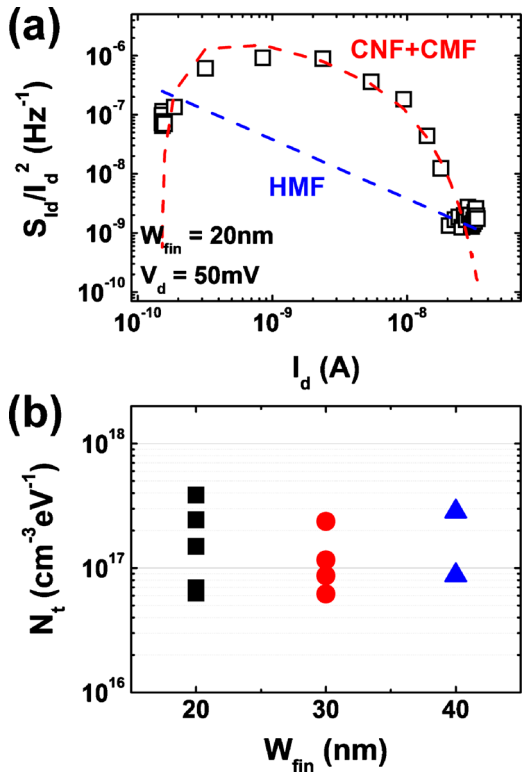

FIG. 2. (Color online) (a) $\log(S_{Id}/I_d^2)-\log(I_d)$ was compared with the CNF+CMF and the HMF model for $W_{fin}=20$ nm. (b) Extracted volume trap density (N_t) of JLTs with different W_{fin}.

in JLTs is affected by trapping/release of carriers even though the conduction takes mostly place in the bulk of the devices. Using the Eqs. (2) and (3), N_t and α_C can be calculated, providing the information on the quality of the oxide interface and the mobility fluctuations by the trapped charges, respectively. The calculated N_t values range from 6×10^{16} to 3×10^{17} cm^{-3} eV^{-1} with $\lambda=1\times10^{-8}$ cm [Fig. 2(b)].[11] These values are similar to those typical in state-of-the-art bulk transistors and considerably smaller than in high-k MOSFETs where $N_t=10^{19}-10^{20}$ cm^{-3} eV^{-1}.[12–14] The value of α_C ranges from 1.1×10^4 to 5.1×10^5 V s/C, indicating that CMF play an important role in the high current region.[11] It can be assumed that these mobility fluctuations are due to Coulombic scattering by charged traps.

In spite of the good interpretation of the CNF+CMF model for the JLTs, it is difficult to understand the effect of traps at the oxide-semiconductor interface in subthreshold region. Because the silicon-gate oxide interfaces are depleted in that regime, and the conduction path is in the center of the nanowire, away from the gate oxide interfaces. A possible explanation is the fluctuation of the channel thickness when the device is partially depleted. This effect arises from the presence of Shockley–Read–Hall generation/recombination centers in the Debye transition region between the neutral channel and the depletion region.[15] This effect has been observed in junction FETs or in four-gate FETs (G^4-FETs).[16,17] Fluctuations of the depleted region can give rise to the generation-recombination (g-r) noise that is characterized by a Lorentzian spectral distribution. When the noise power plotted as a function of V_g, the g-r noise component reaches a peak near threshold as shown in Fig. 3(a).[18,19] When $V_g > V_{fb}$, on the other hand, the depletion region disappears which will decrease the g-r noise in spite of the presence of

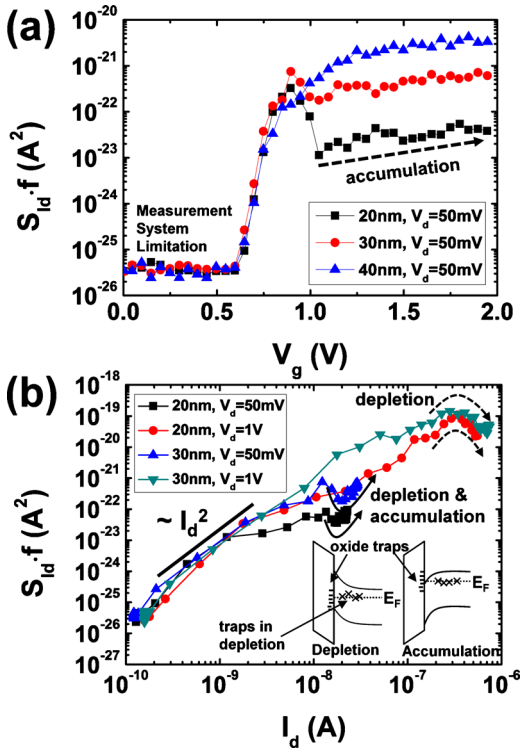

FIG. 3. (Color online) Drain current noise power ($S_{Id}\cdot f$) as a function of (a) the gate voltage V_g with different W_{fin} and (b) the drain current I_d at V_d =50 mV and 1 V. The inset shows the influence of traps at the oxide interface and in depletion region according to the conduction.

a surface accumulation channel.[20] The accumulation channel contributes to the total noise as a result of fluctuations at the oxide-semiconductor interface. The peak at threshold disappears in wide devices, which might be due to the larger size of the bulk conduction region.

In Fig. 3(b), the LF noises generated by the depletion and the accumulation are compared for the different V_d values. For V_d=50 mV, the noise power increases as I_d^2 below the threshold, however, it rises again for large gate voltages, as it does in Fig. 3(a) due to conduction in the surface accumulation. Such behavior is not observed for the case of V_d =1 V because there exists only partial depletion of the silicon near the drain and no accumulation layer is formed near the drain. Hence, the noise originating from the surface conduction could not be observable.

In conclusion, the LF noise in JLTs was well explained by the CNF+CMF model indicating the trapping and detrapping of charge carriers. The JLT exhibits two kinds of noise sources as far as CNFs are concerned: one is due to channel thickness fluctuations in the depletion region and the other is due to carrier concentration fluctuation at the oxide-semiconductor interface in the accumulation region. The relative contribution of the noise sources in JLTs might be a diagnostic index for the quality of the JLTs such as the uniformity of the line width of the channel.

This work has been partly supported by European project SQWIRE under Grant Agreement No. 257111, National Research Foundation of Korea (NRF) grant (Converging Research Center program, Grant No. 2010K000981, WCU Grant No. R32-2008-000-10082-0, GRL Grant No. M6060500007-06A0500-00710, 2005-2002369), CNRS-KIST LIA collaboration, Nanoscience Foundation, Science Foundation Ireland under Grant No. 05/IN/I888, and European Community (EC) Seventh Framework Program through the Networks of Excellence NANOSIL and EUROSOI+ under Contract Nos. 216171 and 216373.

[1]F. N. Hooge, IEEE Trans. Electron Devices **41**, 1926 (1994).
[2]A. L. McWhorter, *Semiconductor Surface Physics* (University of Pennsylvania, Philadelphia, 1957), pp. 207–228.
[3]L. K. J. Vandamme and M. Macucci, AIP Conf. Proc. **800**, 436 (2005).
[4]E. Simoen, A. Mercha, C. Claeys, and N. Lukyanchikova, Solid-State Electron. **51**, 16 (2007).
[5]G. Ghibaudo, O. Roux, C. H. Nguyen-Duc, F. Balestra, and J. Brini, Phys. Status Solidi A **124**, 571 (1991).
[6]C. W. Lee, A. Afzalian, N. Dehdashti Akhavan, R. Yan, I. Ferain, and J. P. Colinge, Appl. Phys. Lett. **94**, 053511 (2009).
[7]J. P. Colinge, C. W. Lee, A. Afzalian, N. Dehdashti Akhavan, R. Yan, I. Ferain, P. Razavi, B. O'Neill, A. Blake, M. White, A. M. Kelleher, B. McCarthy, and R. Murphy, Nat. Nanotechnol. **5**, 225 (2010).
[8]J. P. Colinge, C. W. Lee, I. Ferain, N. Dehdashti Akhavan, R. Yan, P. Razavi, R. Yu, A. N. Nazarov, and R. T. Doria, Appl. Phys. Lett. **96**, 073510 (2010).
[9]C. W. Lee, A. N. Nazarov, I. Ferain, N. Dehdashti Akhavan, R. Yan, P. Razavi, R. Yu, R. T. Doria, and J. P. Colinge, Appl. Phys. Lett. **96**, 102106 (2010).
[10]K. K. Hung, P. K. Ko, C. Hu, and Y. C. Cheng, IEEE Trans. Electron Devices **37**, 654 (1990).
[11]M. V. Haartman and M. Östling, *Low-frequency Noise In advanced MOS Devices* (Springer, New York, 2007).
[12]G. Ghibaudo and T. Boutchacha, Microelectron. Reliab. **42**, 573 (2002).
[13]D. Jang, J. W. Lee, K. Tachi, L. Montes, T. Ernst, G. T. Kim, and G. Ghibaudo, Appl. Phys. Lett. **97**, 073505 (2010).
[14]P. Magnone, F. Crupi, G. Giusi, C. Pace, E. Simoen, C. Claeys, L. Pantisano, D. Maji, V. R. Rao, and P. Srinivasan, IEEE Trans. Device Mater. Reliab. **9**, 180 (2009).
[15]S. H. Ng and C. Surya, Solid-State Electron. **35**, 1803 (1992).
[16]J. A. J. Tejada, A. L. Rodriguez, A. Godoy, J. A. L. Villanueva, F. M. Gomez-Campos, and S. Rodriguez-Bolivar, IEEE Trans. Electron Devices **55**, 896 (2008).
[17]K. Kandiah and F. Whiting, Solid-State Electron. **21**, 1079 (1978).
[18]S. Hayat and B. K. Jones, Semicond. Sci. Technol. **2**, 732 (1987).
[19]B. K. Jones and G. P. Taylor, Solid-State Electron. **35**, 1285 (1992).
[20]K. Akarvardar, B. M. Dufrene, S. Cristoloveanu, P. Gentil, B. J. Blalock, and M. M. Mojarradi, IEEE Trans. Electron Devices **53**, 829 (2006).